

Above-Threshold Dissociation of H_2^+ in Intense Laser FieldsA. Giusti-Suzor,^(a) X. He, and O. Atabek*Laboratoire de Photophysique Moléculaire, Université Paris-Sud, 91405 Orsay, France*

F. H. Mies

National Institute of Standards and Technology, Gaithersburg, Maryland 20899

(Received 7 July 1989)

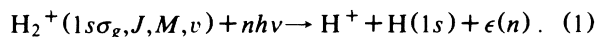
We present nonperturbative, time-independent calculations of the photodissociation rate of H_2^+ in intense laser fields. The energy distribution of the protons consists of a sequence of peaks evenly spaced by half the photon energy, all of equal width but of varying heights. They result from multiphoton absorption above the dissociation threshold, with equal sharing of the excess photon energy between H and H^+ . Surprisingly, the distribution of higher-energy peaks decreases with increasing intensity, due to stimulated free-free emission of the dissociating fragments. We also predict a sharp angular distribution of the protons along the electric field vector of a linear polarized laser.

PACS numbers: 33.80.Gj, 33.80.Wz, 34.50.Rk

It is well demonstrated that multiphoton transitions in intense laser fields may radically change the dynamics of electron-ion collisions and half collisions (photoionization). In particular, the process of above-threshold ionization (ATI), in which free-free photon absorption takes place once the electron is already in the ionization continuum, has been actively studied both experimentally¹ and theoretically,² mostly in atoms but also in a few molecular systems.³⁻⁵ The experimental signature of this process is the appearance of successive peaks, evenly separated by one quantum of photon energy, in the kinetic-energy distribution of ejected photoelectrons.

We address the analogous half-collision process of above-threshold dissociation (ATD) during the photodissociation of a diatomic molecule. In this case the additional quanta of photon energy would appear as evenly spaced peaks in the kinetic-energy spectrum of the atomic photofragments.⁶ Previous wave-packet calculations⁷ of multiphoton dissociation by infrared lasers has already demonstrated this effect for a single electronic state. Although various experiments involving strong-field photoionization of H_2 ^{5,8-10} suggest to us that multiphoton free-free absorptions might be occurring in the dissociation continuum of the product ion H_2^+ , the evidence is by no means unequivocal at this point, and it is our aim in this Letter to encourage more careful examinations of this possibility.

Specifically, we present nonperturbative calculations of the multiphoton photodissociation rate for H_2^+ bound in its ground electronic state



As indicated in Fig. 1 we only consider dissociation via the repulsive $H_2^+(2p\sigma_u)$ electronic state which is asymptotically degenerate with $H_2^+(1s\sigma_g)$. At sufficiently low intensities I , photodissociation will normally proceed via the first energetically accessible continuum state which requires absorption of the least number of photons n_{th} and yields the lowest relative kinetic

energy $\epsilon(n_{th})$. However, even in modest fields $I \approx 10^7$ W/cm², depending on the photon energy $h\nu$ and initial state, we find that absorption of additional photons can easily lead to pathways to dissociation $n > n_{th}$ that are much more favorable than the minimum-energy path. We refer to such processes as above-threshold dissociation to emphasize the similarity with the ATI process.

Our time-independent close-coupled scattering formulation¹¹ is based on defining a finite set of molecule-field channel states involving different photon-number states $|N\rangle$, $|N \pm 1\rangle$, $|N \pm 2\rangle$, We expand the combined molecule-field wave function in the channel states $|d\rangle = |\gamma, n\rangle = |\Lambda JM\rangle \otimes |N - n\rangle$, where $\Lambda \equiv {}^2\Sigma_g^+$ or ${}^2\Sigma_u^+$ and $n = 0, \pm 1, \pm 2$, etc. The quantum numbers J, M designate the total angular momentum of the field-free molecule. At each interatomic distance R , only

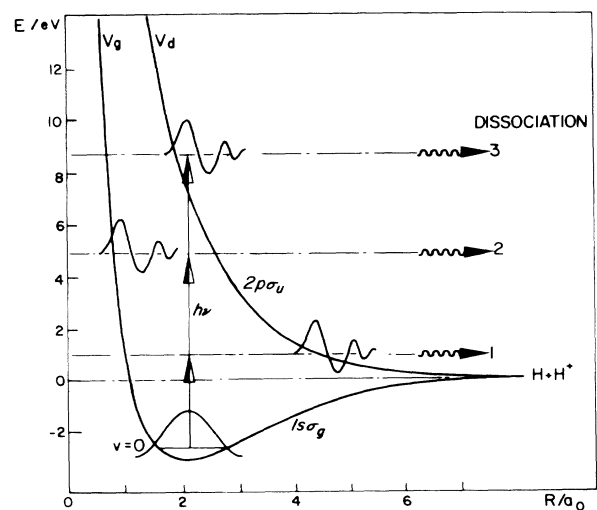


FIG. 1. Potential-energy curves for the ground and first excited states of H_2^+ , with schematic continuum vibrational wave functions after absorption of 1, 2, or 3 photons of wavelength 329.7 nm, from the $v=0$ level of the $1s\sigma_g$ state.

molecule-field channel states whose occupation numbers differ by one photon can be directly coupled by radiative interaction. In the weak-field limit, these couplings simply correspond to the allowed one-photon electronic-rotational transitions $\Lambda, J, M \rightarrow \Lambda', J', M'$ which are well described by perturbation theory and conform to the usual molecular selection rules. However, in the strong-field limit the radial motion associated with the photodissociation of an initially bound vibrational level is best solved in full multichannel close coupling.

In order to develop a proper scattering theory the channel states must be uncoupled at infinite separation of the dissociation fragments. This requirement has two important implications. First, it is critical to choose a gauge for the radiative coupling in which the molecule-field Hamiltonian is asymptotically separable, with eigenvalues subject to laboratory observations. In the dipole approximation the electric field (EF) gauge $\mathbf{E} \cdot \mathbf{r}$ violates this criterion for the $1s\sigma_g \rightarrow 2p\sigma_u$ transition in H_2^+ , and the corresponding transition moment $\mu_{gu}^{\text{EF}}(R)$ derived by Bates¹² asymptotically diverges as $R/2$. As already noted by Chakrabarti, Bhattacharya, and Saha¹³ for HD^+ , it is convenient to use the converged radiative field (RF) gauge $\mathbf{A} \cdot \mathbf{p}$ whenever free-free molecular transitions are involved. The second requirement is that any residual radiative interaction of the atomic and ionic products with the applied laser field must be diagonalized, resulting in field-dressed fragments. To emphasize this important criterion, any quantum number or expectation value capped by an overbar is meant to designate a "field-dressed" property of the system. For instance, the asymptotic energy associated with each channel is $E_d = h\nu(N-n) + \bar{E}_{\text{H}(1\bar{s})} + \bar{E}_{\text{H}^+}$, where $\bar{E}_{\text{H}(1\bar{s})}$ denotes the internal energy of the ground-state hydrogen atom in the field-dressed atomic state $|1\bar{s}\rangle$ appropriately shifted by pondermotive quiver energies and ac-Stark shifts. A set of "field-dressed molecular channel states" $|\bar{a}\rangle$ is obtained by diagonalizing the complete radiative-electronic-rotation part of the total Hamiltonian at each R . Such *adiabatic* molecular states are analogous to the dressed atomic states.¹⁴

Our approach is illustrated in Figs. 1 and 2 for photons of wavelength $\lambda = 329.7$ nm. This λ was chosen to introduce an energetically favorable vertical three-photon transition from the $v=0$ state of $1s\sigma_g$ to the dissociation continuum of the $2p\sigma_u$ state. We combine the two electronic states with up to $n = \pm 5$ photon states $|N-n\rangle$ to form a radiatively coupled set of ten diabatic channel states $|d\rangle = |\gamma, n\rangle$. In Fig. 2 the solid curves correspond to the diagonal elements $U_{d,d}(R)$ of the resultant undressed interaction matrix $\mathbf{U}(R)$. The adiabatic potentials $\bar{U}_{\bar{a},\bar{a}}(R)$ resulting from diagonalization are presented as dotted potential-energy curves in Fig. 2. Of course, the adiabatic channel states $|\bar{a}\rangle$ still experience radial (nonadiabatic) couplings due to the interatomic kinetic-energy operator and either channel basis will yield equivalent solutions to the close-coupled equa-

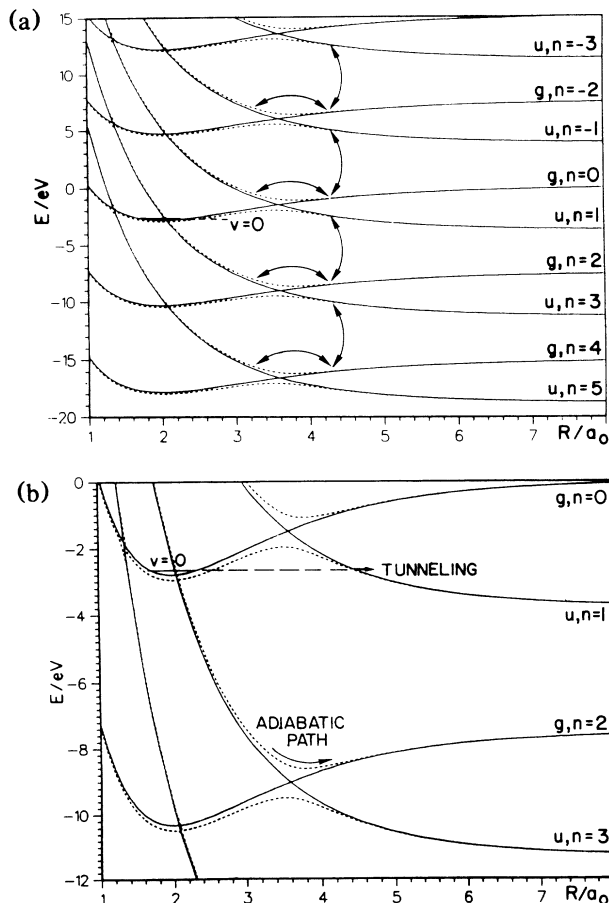


FIG. 2. (a) Potential-energy curves of the two electronic states of H_2^+ in Fig. 1 dressed with ± 5 photons of wavelength 329.7 nm. The solid lines correspond to the ten interacting "diabatic" channel states. Arrows indicate *direct* radiative couplings. The dotted lines represent the field-dressed "adiabatic" curves after diagonalizing the radiative interaction for $I = 1.4 \times 10^{13}$ W/cm². (b) Enlargement of (a) in the region of the curve crossing points which dominate the dissociation process.

tions.

We want to calculate the photodissociation rate $A_r(I, h\nu)$ of the $\text{H}_2^+(r)$ molecule in some prescribed initial bound molecule-field state $|r\rangle$ which is produced by the photoionization of the neutral molecule H_2 . Starting with the diabatic basis, we solve the usual close-coupled equations for a *full* collision using conventional scattering boundary conditions for an outgoing wave associated with each dressed channel state.¹⁵ The *half*-collision amplitude associated with any prescribed vibrational state $|\bar{v}\rangle$ in a given closed channel $|\bar{a}\rangle$ can be projected from the numerical results to yield not only the total broadening, resultant dissociation rate, and associated ac-Stark shift of the initial bound state, but also the branching ratio into specific open channels with varying amounts of absorbed photons. Analysis of our close-coupled results confirm that the adiabatic vibrational lev-

els \bar{v} defined by the adiabatic potentials (dotted curves in Fig. 2) give an excellent quantitative prediction of the location of the laser-induced resonances, which are markedly shifted with respect to the unperturbed diabatic molecular eigenvalues $E_{d,v}$.

The resonance state $|\bar{r}\rangle = |\bar{a}, \bar{v}\rangle$ decays with a total rate, $A_{\bar{r}} = \sum_d A_{\bar{r} \rightarrow d}$, equal to the sum of partial rates into each of the final channel states $|d\rangle = |\gamma, n\rangle$. In our time-independent calculations this yields a Lorentzian lineshape with an intensity-dependent half-width $\Gamma_{\bar{r}} = \hbar A_{\bar{r}}(I)$ determined by the total photodissociation rate. Each partial cross section exhibits a similar Lorentzian shape with the same half-width but a peak intensity proportional to the branching ratio $b_{\bar{r} \rightarrow \bar{d}} = A_{\bar{r} \rightarrow \bar{d}}/A_{\bar{r}}$. This Lorentzian-type behavior has been numerically confirmed over many half-widths $\Gamma_{\bar{r}}$ of displacement from line center $\bar{E}_{\bar{r}}$ which indicates that, in this intensity and wavelength range, the laser-induced predissociation is not sufficient to cause any significant overlap of adjacent vibrational-rotational resonance levels. As can be inferred from Fig. 2(b), the photodissociation is dominated by the three open channels $|d\rangle = |u, n=1\rangle$, $|g, n=2\rangle$, and $|u, n=3\rangle$, with very little likelihood of "tunneling" into the $n=1$ channel. The total width displayed in Fig. 3 for various intensities is found to vary approximately as $\Gamma_{\bar{r}} \propto I^3$. The proton kinetic-energy distribution is shown, consisting of a series of peaks, with heights that are proportional to the branching ratio $b_{\bar{r} \rightarrow d}$. The most striking and somewhat paradoxical result is that, in spite of the I^3 dependence, the $n=3$ channel dominates only for the *lowest* intensity

and is gradually suppressed when the intensity increases, to the profit of the $n=2$ channel.

The explanation of this effect becomes evident in Fig. 2. Once dissociated into the $|u, n=3\rangle$ channel the separating atomic fragments pass through the $|g, n=2\rangle$ and $|u, n=3\rangle$ channel crossing at $R \approx 3.5$ a.u. and the atoms "return" one quanta of photon energy to the radiation field via stimulated emission. This free-free transition can be viewed as a kind of dissociative bremsstrahlung, or resonant Raman process. Note in Fig. 3 that, unlike the width, the resonance *shift* is primarily first order in I , as predicted by the adiabatic $|g, 0\rangle$ curve in Fig. 2 which is mainly repulsed downward by direct coupling to the $|u, -1\rangle$ state. The complete implications of these effects are just being explored, but, especially for longer wavelengths, with many adiabatic crossings on the way to dissociation, it would seem that much of the radiation energy is merely "borrowed" from the radiation field to catalyze the initial decay of the resonance, and is subsequently "returned" to the field via stimulated emissions. In fact, considering the adiabatic nature of these crossings, it would appear that the more intense the laser, the less likely the proton energy will be incremented to produce higher-energy peaks.

Each diabatic channel state in Fig. 2 is associated with an averaged rotational state simply taken as $J \approx 0$, $M \approx 0$. Basically, we ignore the $J \rightarrow J \pm 1$ branching and treat the $J \pm 1$ states as perfectly degenerate with J , with a mean rotational line strength. In strong field there is a rapid escalation of the branching, the approximate degeneracy is destroyed, and intermediate sets of rotational channels must be included.¹⁵ A linearly polarized laser will prepare a very nonthermal distribution of ion channel states with $J \gg 0$, $M \approx 0$. The resonances will ultimately branch into open channels dominated by outgoing spherical waves $Y_{J0}(R)$, which are strongly peaked along the electron field vector of the pumping laser. The admixture of $J \gg 0$ states increases with the laser intensity and the angular distribution of the fragments will become sharper. The details of such branching will be presented in further studies. Note that circular polarization, yielding $\Delta M \neq 0$ transitions, will destroy this propensity for spatial distribution peaked along the field. Such a polarization-dependent angular distribution has been observed in two experiments on H_2 ^{5,10} and could be partially due to this optical-pumping effect.

We have assumed that H_2^+ is prepared in a well-defined field-dressed resonance state $|\bar{r}\rangle = |\bar{a}, \bar{v}\rangle$ in the presence of a strong laser field with constant intensity. We are prepared to make a concession to the pulse shape of the laser by performing a subsequent average of the half-width $\langle \Gamma_{\bar{r}}(I) \rangle_{av}$ over the intensity variation, but we are committed to assuming that the laser pulse varies closely compared to typical collision times involved in the dynamics of dissociation. We can also envision a two-color experiment, where the molecular ion is prepared in a well-defined field-free bound state $|\gamma, v\rangle$ with one laser,

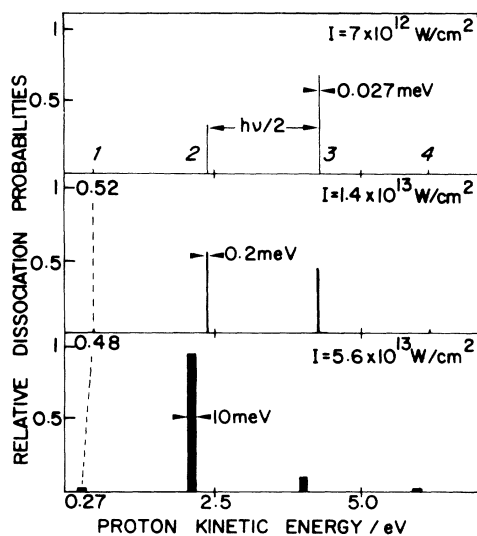


FIG. 3. Schematic representation of the proton energy spectrum in the dissociation process with 329.7 nm and varying intensities. Each peak actually exhibits a Lorentzian shape with a common width indicated in meV for each intensity. Also given (in eV) is the energy of the first peaks. The peak widths and the $n=1$ and 4 peaks are greatly enlarged for clarity.

and subsequently dissociated by a second laser from the initially diabatic resonance state $|r\rangle = |\gamma, n=0\rangle|v\rangle$. Both such rates are well defined by our calculations, and we think that the measurement of proton kinetic energy, simultaneously with the photoelectron energy spectrum in order to know the H_2^+ vibrational distribution as precisely as possible, could lead to interesting distributions strongly dependent on the laser wavelength, intensity, and polarization.

^(a)Also at Laboratoire de Chimie-Physique, 11, rue Pierre et Marie Curie, 75231 Paris, France.

¹P. Agostini, F. Fabre, G. Mainfray, G. Petite, and N. Rahman, *Phys. Rev. Lett.* **42**, 1127 (1979); P. Kruit, J. Kimman, and M. Van der Wiel, *J. Phys. B* **14**, L597 (1981); T. J. McIlrath, P. H. Bucksbaum, R. R. Freeman, and M. Bashkansky, *Phys. Rev. A* **35**, 4611 (1987); R. R. Freeman, P. H. Bucksbaum, H. Milchberg, S. Darack, D. Shumacher, and M. E. Geusic, *Phys. Rev. Lett.* **59**, 1092 (1987); H. G. Muller, H. B. van Linden van den Heuvell, P. Agostini, G. Petite, A. Antonetti, M. Franco, and A. Migus, *Phys. Rev. Lett.* **60**, 565 (1988).

²M. Crance and M. Aymar, *J. Phys. B* **13**, L421 (1980); S. I. Chu and J. Cooper, *Phys. Rev. A* **37**, 2769 (1985); M. Edwards, L. Pan, and L. Armstrong, Jr., *J. Phys. B* **18**, 1927 (1985); Z. Deng and J. H. Eberly, *J. Opt. Soc. Am. B* **2**, 486 (1985); A. Giusti-Suzor and P. Zoller, *Phys. Rev. A* **36**, 5178 (1987); R. M. Potvliege and R. Shakeshaft, *Phys. Rev. A* **38**, 4597 (1988); M. Crance, *J. Phys. B* **21**, 2697 (1988); F. H. M. Faisal, P. Scanzano, and J. Zaremba, *J. Phys. B* **22**, L183 (1989).

³D. Normand, C. Cornaggia, and J. Morellec, *J. Phys. B* **19**, 2881 (1986).

⁴J. W. J. Verschuur and H. B. van Linden van den Heuvell, *Phys. Rev. A* **40**, 4383 (1989).

⁵P. H. Bucksbaum and L. D. Nordam (to be published).

⁶N. K. Rahman, *J. Phys. (Paris), Colloq.* **46**, C1-249 (1985).

⁷R. Heather and H. Metiu, *J. Chem. Phys.* **88**, 5495 (1988).

⁸C. Cornaggia, D. Normand, J. Morellec, G. Mainfray, and C. Manus, *Phys. Rev. A* **34**, 807 (1986).

⁹D. C. Humm, T. Sherlock, K. Ng, J. Mazumder, and M. H. Nayfeh (to be published).

¹⁰K. Codling, L. J. Frasinski, and P. A. Hather, *J. Phys. B* **21**, L433 (1988).

¹¹T. F. George, *J. Phys. Chem.* **86**, 10 (1982); A. D. Bandrauk and G. Turcotte, *J. Phys. Chem.* **87**, 5098 (1983); F. H. Mies, in *Theoretical Chemistry: Advances and Perspectives*, edited by D. Henderson (Academic, New York, 1981), Vol. 6B, p. 124, and references therein; see also X. He, O. Atabek, and A. Giusti-Suzor, *Phys. Rev. A* **38**, 5586 (1988), where a variant of the present method (with *complex rotation* of the nuclear coordinate) was used for a preliminary study of the *total* ATD rate, giving results in perfect agreement with the present ones.

¹²D. R. Bates, *J. Chem. Phys.* **19**, 1122 (1951).

¹³M. K. Chakrabarti, S. S. Bhattacharyya, and S. Saha, *J. Phys. B* **21**, 3717 (1988); *J. Chem. Phys.* **87**, 6284 (1987); *Chem. Phys. Lett.* **113**, 492 (1985).

¹⁴C. Cohen-Tannoudji and S. Haroche, *J. Phys. (Paris)* **30**, 125 (1969); **30**, 153 (1969); C. Cohen-Tannoudji and S. Reynaud, *J. Phys. B* **10**, 345 (1977).

¹⁵P. L. DeVries and T. F. George, *Phys. Rev. A* **18**, 1751 (1978); P. S. Julienne and F. H. Mies, *Phys. Rev. A* **25**, 3399 (1982).